

Coordination field analysis of rare earth complexes with triangular symmetry*

FAN Yingfang (范英芳)**,

(State Key Laboratory of Coordination Chemistry, Institute of Coordination Chemistry,
Nanjing University, Nanjing 210093, China)

PAN Dafeng (潘大丰)

(Shanxi Academy of Agricultural Sciences, Taiyuan 030031, China)

and YANG Pin (杨 频)***

(Institute of Molecular Science, Shanxi University, Taiyuan 030006, China)

Received November 18, 1996

Abstract The calculation of the complex matrixes in odd triangular symmetry was accomplished. The configurations of the coordination unit with various triangular symmetries and different ligand numbers were discussed. On the basis of the double-sphere coordination point-charge (DSCPCF) model, the detailed forms of the DSCPCF parameters B_m^k and the expressions of the perturbation matrix elements in triangular field (D_3 , D_{3h} , D_{3d}) were derived. Thereby, the calculation scheme of coordination field perturbation energy of the rare earth complexes with triangular symmetry was constructed. After the calculation scheme was programmed, the Stark energies of the crystalline $TbAl_3(BO_3)_4$ were calculated. The results were considerably close to the experimental values.

Keywords: triangular field, rare earth complexes, coordination field theory, spectral analysis.

In order to investigate further the coordination behavior and the structure-property relationship of rare earth metal and transition metal complexes, Yang Pin proposed the double-sphere coordination point-charge (DSCPCF) model^[1] and applied it to the calculation of the coordination field perturbation energies of transition metal complexes, as well as biological and drug complexes. The model is satisfactorily successful especially in the spectral analysis of the rare earth complexes^[2]. This is quite significant for developing the crystal field theory, exploring the magnetic and electrical properties and luminescence mechanism of rare earth complexes, as well as for looking for new kinds of optical and magnetic materials and for the applications of the ionic spectral probes, etc. In recent years, we have already made systematical researches on tetragonal and diagonal fields^[3-5]; but those on odd triangular field, one of the main coordination forms, met with a lot of difficulty in the construction of the whole mathematical mode owing to involving the treatment of complex matrixes. Up to now no complete theoretical analysis of it has been found in literature. In most cases, the crystal field parameters B_m^k are treated as the freely adjustable parameters. In the present work, we have applied for the first time the DSCPCF model for the coordination field analysis to rare earth complexes with triangular symmetry. By this model, the

* Project supported by the National Natural Science Foundation of China.

** Present address: Institute of Molecular Science, Shanxi University, Taiyuan 030006, China.

*** To whom correspondence should be addressed.

practical configurations of the complex unit in crystallographic structure are adopted to calculate the crystal field parameters and the coordination field splitting energies and only the effective charges of ligand atoms are treated as the adjustable parameters. Based on the DSCPCF model, we systematically derived the coordination field perturbation matrix elements with the irreducible tensor operator method in D_3 -field and designed the computer program that can be used in the spectral analysis of the rare earth metal complexes with triangular symmetry. The calculation can simulate the Stark energies of $\text{TbAl}_3(\text{BO}_3)_4$ crystalline. The result shows that our method has a good precision and the calculation is concise, rapid and clear in physical meanings.

1 Coordination field potential function and expressions of DSCPCF parameters in the triangular field

The theoretical analysis method and the description of the DSCPCF model can be referred to refs. [2] and [5]. In triangular field (D_3 , D_{3d} , C_{3v}), the tensor operator form of the coordination field perturbation energy level is

$$\hat{H}_{\text{cf}} = B_0^2 C_0^2 + B_0^4 C_0^4 + B_3^4 (C_3^4 - C_{-3}^4) + B_0^6 C_0^6 + B_3^6 (C_3^6 - C_{-3}^6) + B_6^6 (C_6^6 + C_{-6}^6). \quad (1)$$

In order to make the crystal field parameters be real functions, an appropriate set of axes should be selected. Considering a complex unit with D_3 symmetry, Z -axis is placed in the direction of the main axis C_3 ; X -axis is in the plane perpendicular to the crystal c at -30° from the crystal axis a ; and Y -axis is the second-order axis C_2 , consistent with the prescription in refs. [6, 7]. The general expressions of the DSCPCF parameters B_m^k in the D_3 -field can be obtained as follows:

$$B_0^2 = 1/2 \langle r^2 \rangle \sum_j (q_j / r_j^3 - Z_j^* / R_j^3) (3 \cos^2 \Theta_j - 1),$$

$$B_0^4 = 1/8 \langle r^4 \rangle \sum_j (q_j / r_j^5 - Z_j^* / R_j^5) (35 \cos^4 \Theta_j - 30 \cos^2 \Theta_j + 3), \quad (2)$$

$$B_3^4 = -\sqrt{35}/4 \langle r^4 \rangle \sum_j (q_j / r_j^5 - Z_j^* / R_j^5) \cos 3 \Phi_j \sin^3 \Theta_j,$$

$$B_0^6 = 1/16 \langle r^6 \rangle \sum_j (q_j / r_j^7 - Z_j^* / R_j^7) (231 \cos^6 \Theta_j - 315 \cos^4 \Theta_j + 105 \cos^2 \Theta_j - 5) \quad (3)$$

$$B_3^6 = -\sqrt{105}/16 \langle r^6 \rangle \sum_j (q_j / r_j^7 - Z_j^* / R_j^7) \cos \Theta_j (11 \cos^2 \Theta_j - 3) \sin^3 \Theta_j \cos 3 \Phi_j,$$

$$B_6^6 = \sqrt{231}/32 \langle r^6 \rangle \sum_j (q_j / r_j^7 - Z_j^* / R_j^7) \cos 6 \Phi_j \sin^6 \Theta_j. \quad (4)$$

For a concrete rare earth complex with various configurations of triangular symmetry and different ligand numbers, the spherical coordinates of ligand atoms can be substituted and the corresponding expressions of B_m^k can be obtained.

For a complex unit [$\text{R}_E\text{A}_6\text{B}_3\text{C}_3\text{D}_2$] as shown in fig. 1, the ligand number around the rare earth central ion R_E is fourteen, and four types of ligand atoms are concerned, which are shown as follows:

$$\begin{aligned} A_1(R_A, \Theta_A, \pi/6 + \alpha), & \quad A_2(R_A, \Theta_A, 5\pi/6 + \alpha), \\ A_3(R_A, \Theta_A, 9\pi/6 + \alpha), & \quad A_4(R_A, \pi - \Theta_A, \pi/6 - \alpha), \\ A_5(R_A, \pi - \Theta_A, 5\pi/6 - \alpha), & \quad A_6(R_A, \pi - \Theta_A, 9\pi/6 - \alpha), \\ B_1(R_B, \pi/2, \pi/6), & \quad B_2(R_B, \pi/2, 5\pi/6), \end{aligned}$$

$$\begin{aligned} B_3(R_B, \pi/2, -\pi/2), \\ C_2(R_C, \pi/2, -5\pi/6), \\ D_1(R_D, 0, 0), \end{aligned}$$

$$\begin{aligned} C_1(R_C, \pi/2, \pi/2), \\ C_3(R_C, \pi/2, -\pi/6), \\ D_2(R_D, \pi, 0). \end{aligned}$$

In fig. 1, 2α represents the horizontal tortile angle between atoms 1 and 4 of type A in the upside layer and the downside layer. Let $2\varphi_A$ be $\angle A_1-R_E-A$. Then there exists the following relation among the polar angle Θ_A , the tortile angle 2α and the bond angle $2\varphi_A$:

$$\sin\Theta_A \cos\alpha = \cos\varphi_A. \quad (5)$$

The general cases for various triangular symmetry coordination configurations and their different ligand numbers are as follows:

(i) When atoms of type D are removed, the complex unit is of D_3 configuration with 12-ligand number. Furthermore, if $R_A = R_B = R_C$, $Z_A^* = Z_B^* = Z_C^*$ and $2\alpha = \pi/3$, it is of the O_h cubic configuration.

(ii) When atoms of types C and D are removed, it is of D_3 configuration with 9-ligand number. Furthermore, if $2\alpha = 0$, it is of the D_{3h} tricapped trigonal prism configuration.

(iii) When atoms of types B and C are removed, it is of D_3 configuration with 8-ligand number. Furthermore, if $2\alpha = \pi/3$, it is of the D_{3d} bicapped trigonal antiprism configuration; if $2\alpha = 0$, it is of the D_{3h} bicapped trigonal prism configuration.

(iv) When atoms of type A are removed, it is of D_3 configuration with 8-ligand number. Furthermore, if $R_B = R_C$ and $Z_B^* = Z_C^*$, it is of the D_{6h} hexagonal bipyramid configuration.

(v) When atoms of types B and C and atom D_2 are removed, it is of D_3 configuration with 7-ligand number. Furthermore, if $2\alpha = \pi/3$, it is of the C_{3v} monocapped octahedron configuration.

(vi) When atoms of types B, C and D are removed, it is of D_3 configuration with 6-ligand number. Furthermore, if $2\alpha = \pi/3$, it is of the D_{3d} trigonal antiprism configuration; if $2\alpha = 0$, it is of the D_{3h} trigonal prism configuration.

(vii) When atoms of types B and C as well atoms A_4, A_5 and A_6 are removed, it is of D_{3h} trigonal bipyramid configuration with 7-ligand number.

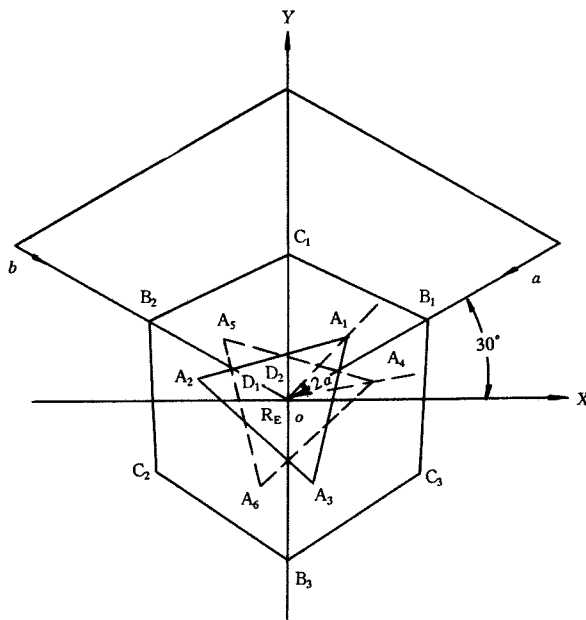


Fig. 1. Projection of the Z-axis of the complex unit $[R_E A_6 B_3 C_3 D_2]$.

2 Basic vectors and coordination field perturbation matrix elements

For the $4f^N$ electron configuration, the coupling scheme of Russell-Saunders is adopted. The states of D_3 -point group are classified according to the point group chain relation $SO^*(3) \supset O^* \supset D_3^*$. For the corresponding complex ion the D_3 -group basic vectors of the irreducible representations $|(\gamma SL)J\tau\Gamma P\rho\rangle$ are expressed as the linear combination of the L - S coupling wave functions $|(\gamma SL)JM\rangle$, in which J , Γ and P are the irreducible representational symbols of the $SO^*(3)$, O^* , and D_3^* point groups, respectively, and ρ is a row index of P . They can be worked out in two steps:

$$\begin{aligned} \text{(i)} \quad SO(3) \rightarrow O: |J\tau\Gamma\gamma\rangle &= \sum_M S_{M, \tau\Gamma}^J |JM\rangle, \\ \text{(ii)} \quad O \rightarrow D_3: |J\tau\Gamma P\rho\rangle &= \sum_\gamma S_{\gamma, P\rho}^\Gamma |J\tau\Gamma\gamma\rangle \\ &= \sum_M \sum_\gamma S_{M, \tau\Gamma}^J S_{\gamma, P\rho}^\Gamma |JM\rangle = \sum_M S_{M, P\rho}^{J, \tau\Gamma} |JM\rangle, \end{aligned} \quad (6)$$

in which, the final transformation coefficients $S_{M, P\rho}^{J, \tau\Gamma} = \sum_\gamma S_{M, \tau\Gamma}^J S_{\gamma, P\rho}^\Gamma$, which can be obtained from refs. [6, 7]. For the case with a half of integer, J , the complex coupling coefficients appear in the irreducible representation ϵ'' .

For the f^N configuration, the coordination field perturbation matrix elements in D_3 -field are expressed as

$$\begin{aligned} &\langle (\gamma SL)J\tau\Gamma P\rho | \hat{H}_{cf} | (\gamma' S'L')J'\tau'\Gamma'P'\rho'\rangle \\ &= \sum_{M, M'} S_{M, P\rho}^{J, \tau\Gamma} S_{M', P'\rho'}^{J', \tau'\Gamma'} \cdot \langle (\gamma SL)JM | \hat{H}_{cf} | (\gamma' S'L')J'M'\rangle \cdot \delta_{PP'} \cdot \delta_{\rho\rho'}. \end{aligned} \quad (7)$$

From formula (7) it is known that only the matrix elements for the basic vectors belonging to the same irreducible representation and the same row of the point group may be equal to nonzero. The matrix elements on the right-hand side of the above equation can be simplified according to the properties of tensor operator and the Wigner-Eckart theorem^[5] and then the expressions are easily obtained.

Let us define six parameters for T_m^k as follows:

$$\begin{aligned} T_0^2 &= aA_0^2 \langle r^2 \rangle, & T_0^4 &= bA_0^4 \langle r^4 \rangle, & T_0^6 &= cA_0^6 \langle r^6 \rangle, \\ T_3^4 &= \sqrt{70}bA_3^4 \langle r^4 \rangle, & T_3^6 &= \sqrt{210}cA_3^6 \langle r^6 \rangle, & T_6^6 &= \sqrt{231}cA_6^6 \langle r^6 \rangle. \end{aligned} \quad (8)$$

And thus the calculation of the coordination field matrix elements has been greatly simplified. For the rare earth ion with $4f^N$ ($N=1-13$) configuration, the obtained nonzero matrix element representations in D_3 -field of various multiplets are only the linear combinations of the above six parameters of T_m^k ($k=2, 4, 6; m=0, \pm 3, \pm 6$), i. e.

$$\langle f^N(\gamma SL)J\Gamma P | \hat{H}_{cf} | f^N(\gamma' S'L')J'\Gamma'P \rangle = \sum_{k, m} f_m^k T_m^k. \quad (9)$$

Here, the linear combination coefficients f_m^k are not related to the classification indices γSL of terms and can be tabulated according to J values (table 1). The three coefficients a , b and c involved in the T_m^k parameters are in relation to the specific term of the defined electron configuration (table 2).

Table 1 Linear combination coefficients in the representations of coordination field perturbation matrix elements in D_3 -field for $J = 3$ and $9/2$

	f_0^2	f_0^4	f_0^6	f_3^4	f_3^6	f_6^6
$\langle 3T_2\alpha_1 \hat{H}_{cf} 3T_2\alpha_1 \rangle$	10	-9	-18	0	0	-36
$\langle 3A_2\alpha_2 \hat{H}_{cf} 3A_2\alpha_2 \rangle$	0	-14	192	4	16	16
$\langle 3T_1\alpha_2 \hat{H}_{cf} 3T_1\alpha_2 \rangle$	2	-13	150	-4	-16	20
$\langle 3A_2\alpha_2 \hat{H}_{cf} 3T_1\alpha_2 \rangle$	$4\sqrt{5}$	$2\sqrt{5}$	$-84\sqrt{5}$	$1/\sqrt{5}$	$4/\sqrt{5}$	$8\sqrt{5}$
$\langle 3T_1\epsilon \hat{H}_{cf} 3T_1\epsilon \rangle$	-1	17	45	-1	18	0
$\langle 3T_2\epsilon \hat{H}_{cf} 3T_2\epsilon \rangle$	-5	1	-207	1	-18	0
$\langle 9/2E'\epsilon' \hat{H}_{cf} 9/2E'\epsilon' \rangle$	0	196	-384	56	48	-32
$\langle 9/2(1)U'\epsilon' \hat{H}_{cf} 9/2(1)U'\epsilon' \rangle$	-3	201	-117	-12	0	42
$\langle 9/2(2)U'\epsilon' \hat{H}_{cf} 9/2(2)U'\epsilon' \rangle$	-15	-19	15	-44	-48	-10
$\langle 9/2E'\epsilon' \hat{H}_{cf} 9/2(1)U'\epsilon' \rangle$	$-2\sqrt{42}$	$-30\sqrt{42}$	$48\sqrt{42}$	$3\sqrt{42}$	$24/7\sqrt{42}$	$-2\sqrt{42}$
$\langle 9/2E'\epsilon' \hat{H}_{cf} 9/2(2)U'\epsilon' \rangle$	$-6\sqrt{2}$	$-170\sqrt{2}$	$-168\sqrt{2}$	$17\sqrt{2}$	$12\sqrt{2}$	$22\sqrt{2}$
$\langle 9/2(1)U'\epsilon' \hat{H}_{cf} 9/2(2)U'\epsilon' \rangle$	$-\sqrt{21}$	$-45\sqrt{21}$	$-93\sqrt{21}$	$-36/7\sqrt{21}$	$-24/7\sqrt{21}$	$-4\sqrt{21}$
$\langle 9/2(1)U'\epsilon'' \hat{H}_{cf} 9/2(1)U'\epsilon'' \rangle$	3	-159	261	24	-24	-30
$\langle 9/2(2)U'\epsilon'' \hat{H}_{cf} 9/2(2)U'\epsilon'' \rangle$	15	-219	225	-24	24	30
$\langle 9/2(1)U'\epsilon'' \hat{H}_{cf} 9/2(2)U'\epsilon'' \rangle$	$\sqrt{21}$	$-5\sqrt{21}$	$-3\sqrt{21}$	$-64/7\sqrt{21}$	$64/7\sqrt{21}$	$-4\sqrt{21}$
	$4i\sqrt{42}$	$-20i\sqrt{42}$	$-12i\sqrt{42}$	$2i\sqrt{42}$	$-2i\sqrt{42}$	$-4/7i\sqrt{42}$

Table 2 Matrix element coefficients a , b and c of the configurations f^6 and f^8 in D_3 -field

J	$2S+1L_J$	a	b	c
0	7F_0	0	0	0
	$(3)^5D_0$	0	0	0
1	$(3)^5D_1$	-11/350	0	0
	7F_1	1/10	0	0
2	$(3)^5D_2$	33/3 430	-295/101 871	0
	7F_2	-11/210	1/189	0
3	7F_3	-1/180	-1/594	5/46 332
	$(3)^5D_3$	-11/4 900	295/58 212	0
4	7F_4	-1/1 540	-23/45 738	5/56 628
	$(3)^5D_4$	11/6 860	-295/1 222 452	0
5	7F_5	-1/720	-1/594	-5/92 664
6	7F_6	-1/528	1/13 068	5/2 038 608
	5L_6	0	-19/155 584	-115/18 203 328
1-2	7F_1 - 7F_2	1/30	0	0

3 Coordination field perturbation energies of Tb^{3+} in crystalline $TbAl_3(BO_3)_4$

The lanthanide aluminium borates, $LnAl_3(BO_3)_4$, as an unity of nonlinear optical material and self-frequency-doubling laser crystal, have aroused the utmost interest of researchers in recent years^[8,9]. A deep inquiring into the energy distribution and the spectral structure of rare earth ion in such a crystalline is significant in both theoretical study and practical application. Corller-Walrand *et al.* simulated the crystal field effects of $TbAl_3(BO_3)_4$ and $EuAl_3(BO_3)_4$. But the obtained

parameters B_m^k are adjustable and could not really reflect any information on microstructure, such as the charge distribution around the rare earth ion, etc. With the experimental spectral data as the initial information, we calculated the energy level diagram using the above method.

$\text{LnAl}_3(\text{BO}_3)_4$ is all isomorphous with huntite $\text{CaMg}_3(\text{CO}_3)_4$. Each Ln^{3+} ion is coordinated with six oxygen atoms of the borate anions, forming a D_3 -distorted trigonal prism^[9]. The distortion angle $\alpha = 8.14^\circ$. The coordinates of the six ligand oxygen atoms in complex unit $[\text{LnO}_6]$ are adopted as that of the six type A atoms in figure 1.

In crystal $\text{Gd}(\text{Eu})\text{Al}_3(\text{BO}_3)_4$, the distance $R_{\text{Eu-O}}$ is 0.234 1 nm and the polar angle Θ_A is obtained from X-ray diffraction experiment to be 53.9° . Referring these values, we slightly adjust them in the simulation according to the theoretical analysis. For $\text{TbAl}_3(\text{BO}_3)_4$, the values of the parameters are given below: $R_{\text{Tb-O}} = 0.234$ nm, $\Theta_A = 53.0^\circ$ and $\alpha = 8.14^\circ$. In the calculation, the values of the radial integrals $\langle r^k \rangle$ are: $\langle r^2 \rangle = 0.770a_0^2$, $\langle r^4 \rangle = 1.508a_0^4$, $\langle r^6 \rangle = 6.300a_0^6$, and for the Tb^{3+} ion, $Z_M^* = 22.65$ e. Through simulating the experimental energies using the DSCPCF model, the effective charges of ligand atoms are $Z_O^* = 2.226$ e, whereas in PCF calculation the effective net negative charges of ligands are $Q = -1.165$ e. The crystal parameters B_m^k calculated from the DSCPCF and PCF models and their ratio values R_m^k are listed in table 3. The coordination field perturbation splittings, energies and the experimental values are listed simultaneously in table 4 so as to compare them.

Table 3 Crystal parameters B_m^k and ratio values $R_m^k = B_m^k(\text{DSCPCF})/B_m^k(\text{PCF})$ of $\text{TbAl}_3(\text{BO}_3)_4$

B_m^k/cm^{-1}	B_0^2	B_0^4	B_2^4	B_0^6	B_2^6	B_6^6
DSCPCF	-354.2	1355.1	-620.6	-272.6	-129.8	131.9
PCF	-591.3	560.1	-256.5	-49.0	-23.4	23.7
R_m^k	0.599	2.419	2.419	5.563	5.547	5.565

Table 4 Coordination field perturbation energies of Tb^{3+} in crystal $\text{TbAl}_3(\text{BO}_3)_4$

Multiplet (energy)	$E_{\text{exp.}}$	DSCPCF calculation			PCF calculation		
		IR rep.	splitting	$E_{\text{calc.}}$	IR rep.	splitting	$E_{\text{calc.}}$
7F_6 (280)	0	T_1a_2	-249.3	30.7	T_1a_2	-249.6	30.4
	0	(1) T_2a_1	-249.1	30.9	(1) T_2a_1	-249.5	30.5
	210	A_1a_1	-51.3	228.7	(1) T_2e	-17.2	262.8
	272	T_1e	-40.3	239.7	T_1e	41.1	321.1
	275	(1) T_2e	-19.1	260.9	Ee	48.0	328.0
	-	A_2a_2	96.9	376.9	A_1a_1	51.9	331.9
	434	(2) T_2e	109.9	389.9	(2) T_2e	63.6	343.6
	-	(2) T_2a_1	115.9	395.9	A_2a_2	73.2	353.2
7F_5 (2267)	472	Ee	118.0	398.0	(2) T_2a_1	102.9	382.9
	2144	(2) T_1e	-132.2	2134.8	(2) T_1e	-78.8	2188.2
	2166	T_2a_1	-78.4	2188.6	T_2a_1	-27.4	2239.6
	2190	(1) T_1a_2	-56.4	2210.6	(1) T_1a_2	-24.9	2242.1
	2247	T_2e	-7.3	2259.7	Ee	-17.9	2249.1
	2287	Ee	54.0	2321.0	T_2e	-10.3	2256.7

(To be continued on the next page)

(Continued)

Multiplet (energy)	$E_{exp.}$	DSCPCF calculation			PCF calculation		
		IR rep.	splitting	$E_{calc.}$	IR rep.	splitting	$E_{calc.}$
7F_4 (3 603)	2 393	(1) $T_1\epsilon$	98.1	2 365.1	(1) $T_1\epsilon$	83.7	2 350.7
	2 443	(2) T_1a_2	109.4	2 376.4	(2) T_1a_2	98.9	2 365.9
	3 448	A_1a_1	-146.7	3 456.3	A_1a_1	-66.0	3 537.0
	3 486	$T_1\epsilon$	-92.9	3 510.1	T_1a_2	-51.2	3 551.8
	3 548	T_1a_2	-90.8	3 512.2	$T_1\epsilon$	-27.8	3 575.2
	3 590	$E\epsilon$	-6.1	3 596.9	$E\epsilon$	-1.7	3 601.3
7F_3 (4 587)	3 723	$T_2\epsilon$	136.1	3 739.1	$T_2\epsilon$	51.3	3 654.3
	3 774	T_2a_1	163.3	3 766.3	T_2a_1	73.6	3 676.6
	4 539	$T_1\epsilon$	-54.5	4 532.5	$T_1\epsilon$	-23.8	4 563.2
	4 542	T_1a_2	-4.5	4 582.5	T_1a_2	-14.6	4 572.4
	4 592	$T_2\epsilon$	6.4	4 593.4	$T_2\epsilon$	-12.0	4 575.0
	4 623	T_2a_1	33.0	4 620.0	T_1a_2	40.0	4 627.0
7F_2 (5 319)	4 682	A_2a_2	67.7	4 654.7	A_2a_2	46.2	4 633.2
	5 145	T_2a_1	-166.2	5 152.8	T_2a_1	-115.3	5 203.7
	5 307	$T_2\epsilon$	-22.1	5 296.9	$T_2\epsilon$	14.2	5 333.2
7F_1 (5 749)	5 418	$E\epsilon$	105.1	5 424.1	$E\epsilon$	43.5	5 362.5
	5 661	T_1a_2	-70.8	5 678.2	T_1a_2	-118.3	5 630.7
7F_0	5 793	$T_1\epsilon$	35.4	5 784.4	$T_1\epsilon$	59.1	5 808.1
	5 993	A_1a_1	0.0	5 993.0	A_1a_1	0.0	5 993.0
σ			28.2			52.2	

4 Discussion and conclusion

In the $TbAl_3(BO_3)_4$ crystal, there exists a relatively strong crystal field for the Tb^{3+} . The DSCPCF splitting distances of the multiplet energies 7F_6 , 7F_5 , 7F_4 , 7F_3 , 7F_2 and 7F_1 are 367.3, 241.6, 310.0, 122.2, 271.3 and 106.2 cm^{-1} respectively, whereas the PCF splitting distances are 352.5, 177.7, 139.6, 70.0, 158.8 and 177.4 cm^{-1} respectively. The corresponding experimental values are 472, 299, 326, 143, 273 and 132 cm^{-1} respectively. The ligand atoms in complex unit $[TbO_6]$ possess relatively big effective nuclear charge Z_j^* ($=2.226 e$) and net negative charge $-Q_j$ ($=1.165 e$). All this information shows that in the interaction between the ligand and ion Tb^{3+} there exists a relatively strong covalent component part. From table 4, it may be seen that for the $4f^8$ system in a triangular field, the DSCPCF model and the PCF model gave roughly the same energy level structure, but root-mean-square deviation between the former and the experiment is much smaller than that of the latter. The greatest difference between the two models is that the PCF splitting energy is too large when the value of J is small ($J=1$), whereas it is too small when the value of J is large ($J \geq 2$). The result obtained from the DSCPCF model is closer to the practical situation. This is because the DSCPCF model is better to describe the coordination field effect compared with the PCF model. From the whole parameters B_m^k (table 3) we can see that the difference between the two models is very clear. Compared with the PCF model, the DSCPCF model made B_0^2 decrease slightly, B_m^4 increase by 2.4 times and especially B_m^6 increase by more than 5 times. This correction is of remarkable superiority for simulating the spectra of the multiplets with relatively large J values. In general, for the multiplets with large J

values greater progress in the result of the DSCPCF calculation can be made compared with that of the PCF calculation^[2]. This conclusion is also suitable for the case of the rare earth complexes with triangular symmetry.

From table 4 it can also be seen that the energies calculated with the DSCPCF model are consistent with the observed data. This shows that the DSCPCF model is effective. In ref. [10], using the parameter simulation method, the B_m^k were treated as free parameters and obtained from the simulation via the experiment, as a result, they cannot reflect the information of the real coordination structure of the crystal, the bonding property, etc. In the present paper, the measured structure data are taken as the starting point and only the effective charge of ligand atoms is as the adjustable parameter, but this new method gives the coordination field energy order similar to that of the previous method. It shows that the B_m^k obtained by the present method have their clear physical meanings. Furthermore, this provides a new method for strictly investigating the theoretical assignment of the triangular field energies according to the transition selection rules of D_3 -group, and has made spade-work for studies on the symmetrical structure of rare earth complexes through the MCD spectra.

References

- 1 Yang Pin, Li Lemin, Double sphere coordination point charge field model and the inhomogeneous Feynman force effect, *Ke-xue Tongbao* (in Chinese), 1982, 27(5): 511.
- 2 Yang Pin, Fan Yingfang, Double sphere coordination point charge field model and some relevant problems, *Transition Met. Chem.*, 1995, 20: 485.
- 3 Fan Yingfang, Yang Pin, Coordination field analysis of the fluorescence spectra of $\text{Eu}(\text{Phen})_2(\text{NO}_3)_3$ and $\text{Eu}(\text{PU})_8(\text{NO}_3)_3$, *J. Phys. Chem.*, 1996, 100(1): 69.
- 4 Yang Pin, Wang Yuekui, Analysis of spectra for Pr(III)- and Tm(III)-2-thenoyltrifluoroacetone piperidine complexes, *Scientia Sinica*, Ser. B, 1987, 30(8): 794.
- 5 Fan Yingfang, Yang Pin, Pan Dafeng *et al.*, Coordination field calculation for the rare earth complexes in the diangular symmetry field, *Science in China*, Ser. B, 1995, 38(4): 401.
- 6 Freeman, A. J., Watson, R. E., Theoretical investigation of some magnetic and spectroscopic properties of rare-earth ions, *Phys. Rev.*, 1962, 127: 2058.
- 7 Zhang Qianer, *Polyhedral Molecular Orbit* (in Chinese), Beijing: Science Press, 1987.
- 8 Tang Aoqing, *Method of Coordination Field Theory* (in Chinese), Beijing: Science Press, 1979.
- 9 Gorller-Walrand, C., Vandavelde, P., Hendrickx, I. *et al.*, A spectroscopic study of the $\text{TbAl}_3(\text{BO}_3)_4$ crystal, *Inorg. Chim. Acta*, 1987, 139: 277.
- 10 Kuroda, R., Mason, S. F., Rosini, C., Crystal structure and single crystal spectra of $\text{Gd}(\text{Eu})\text{Al}_3(\text{BO}_3)_4$, *J. Chem. Soc. Faraday Trans. 2*, 1981, 77: 2125.